Arabian Journal of Chemistry (2017) **10**, S244–S251

King Saud University

Arabian Journal of Chemistry

www.ksu.edu.sa
www.sciencedirect.com

ORIGINAL ARTICLE

Cucumis sativus used as adsorbent for the removal of dyes from aqueous solution

T. Smitha [a], **T. Santhi** [a,*], Ashly Leena Prasad [a], S. Manonmani [b]

[a] *Department of Chemistry, Karpagam University, Coimbatore 641 021, India*
[b] *Department of Chemistry, PSG College of Arts and Science, Coimbatore 641 014, India*

Received 18 August 2011; accepted 23 July 2012
Available online 4 August 2012

KEYWORDS

Cucumis sativus;
Adsorption;
Isotherm;
Kinetics;
Eco friendly

Abstract In this article, the agricultural solid waste, *Cucumis sativus* (RCS) was activated by sulfuric acid (CCS) for removing typical basic dyes, crystal violet (CV) and rhodamine B (RHB) from aqueous solution. The different parameters like effect of concentration, sorbent dosage, contact time and pH were studied. Isotherm data showed that the Langmuir isotherm provided the best correlation for the adsorption of CV and RHB onto RCS and CCS. The kinetic experimental data were well fitted by the pseudo-second-order kinetic model with intraparticle diffusion being one of the rate limiting steps. It can be concluded that *C. sativus*, the eco friendly adsorbent, is expected to be environmentally and economically feasible for the removal of CV and RHB from aqueous solution.

1. Introduction

Waste water from dyeing and finishing operations associated with the textile industry is highly contaminated in both color and organic content. Color removal from textile effluents has been the target of great attention in the last few years, not only because of its potential toxicity, but also due to visibility problems (Voundrias et al., 2002). To protect humans and the receiving ecosystem from contamination, the dyes must be eliminated from the dye containing wastewaters before being released into the environment. Various physicochemical and biological techniques have been employed to remove dyes from waste water. They include membrane filtration, coagulation/flocculation (Mecay et al., 1984), adsorption (Meshko et al., 1998), ion-exchange (Wong et al., 2004), advanced oxidation (Forgacs et al., 2004), and biological treatment (bacterial and fungal biosorption, biodegradation in aerobic or anaerobic conditions) (Kaur et al., 1998). The technical and economical feasibility of each technique is determined by several factors such as dye type, waste water composition, operation costs and generated water products. Also the use of one individual technique is not sufficient to achieve complete discoloration. Therefore dye removal strategies consist of a combination of different techniques.

Amongst various techniques, adsorption is superior in simplicity of design, initial cost, ease of operation and insensitivity to toxic substance. A large number of suitable adsorbents such as activated carbon, polymeric resins or various low cost adsorbents (non modified or modified cellulose biomass, chi-

* Corresponding author. Tel.: +91 04222401661; fax: +91 042226 11146.
E-mail address: ssnilasri@yahoo.co.in (T. Santhi).
Peer review under responsibility of King Saud University.

ELSEVIER Production and hosting by Elsevier

http://dx.doi.org/10.1016/j.arabjc.2012.07.030
1878-5352

tin, bacterial biomass, etc.) have been studied. Identification of a potential dye adsorbent must be in good agreement with its dye binding capacity, its regeneration properties, its requirements and limitations with respect to environmental condition. The valorization of agricultural wastes into valuable materials without generating pollutants is a big challenge and recommended for an industrial sustainable development in order to preserve the environment (Santhi et al., 2010).

Cucumis sativus is a leading commercial crop and a popular home garden vegetable. Commercial cucumber production includes processing types for pickling and fresh market types for slicing. At one season or another, cucumbers may be grown in all regions of India. The peel of *C*. sativus is a segregated waste product, hence it is available free of cost. The aim of the paper is to find out the more suitability and applicability of carbon prepared from *C*. sativus for the uptake of cationic dyes from simulated waste water (Santhi and Manonmani, 2010, 2011). To evaluate the adsorption potential of *C*. sativus leaves for removing dyes from wastewater, crystal violet (CV) and rhodamine B (RH B) were selected as the model cationic dyes. Discharge of CV into the hydrosphere can cause environmental degradation, because CV is readily absorbed into the fish tissue by water exposure and is reduced metabolically by fish to the leuco moiety, leucocrystal violet (LCV). Several studies by the National Toxicology Program reported the carcinogenic and mutagenic effects of crystal violet in rodents. It has also been linked to increased risk of human bladder cancer. The leuco form induces renal, hepatic and lung tumor in mice. In California, rhodamine B is suspected to be carcinogenic and thus products containing it must contain a warning on its label.

2. Materials and methods

2.1. Materials

The commercial grade CV and RH B, models of the cationic dye with molecular formula of $C_{25}H_{30}ClN_3$ and $C_{28}H_{31}ClN_2O_3$ were used in the present study. Crystal violet (color index No. 42555) with molecular weight 407.99 and λ_{max} 584 nm are obtained from Thomas baker (chemicals) Ltd., Mumbai, India and rhodamine B (color index No. 45170) with molecular weight 479.02 and λ_{max} 554 nm are obtained from Qualigens fine chemicals Mumbai, India. The molecular structures are illustrated in Fig. 1. All the chemicals used throughout this study were of analytical-grade reagents and the adsorption experiments were carried out at room temperature (27 ± 2 °C).

2.2. Adsorbent preparation

The fruit peel of *C*. *Sativus* used for the present study was collected from Palamudhir Nilyam, Coimbatore. The fruit peel was crushed and dried in an oven and used as a raw adsorbent (RCS). The oven dried peel of the adsorbent was treated with conc. H_2SO_4 for 12 h and was washed thoroughly with distilled water till it attained neutral pH and soaked in 2% $NaHCO_3$, for overnight in order to remove any excess of acid present. Then the material was washed with distilled water and dried. The material thus obtained was designated into activated carbon (CCS). The materials were sieved to get different geometrical sizes such as 75–125, 125–250 and 250–500 mμm.

2.3. Characterization of prepared adsorbents

Determination of zero point charge (pH_{zpc}) was done to investigate the surface charge of both chemically and microwave activated adsorbents at different solution pH.

2.4. Dye uptake experiments

The adsorption experiments were carried out in a batch process to evaluate the effect of pH, contact time, adsorbent dose, adsorption kinetics, adsorption isotherm of CV and RH B onto RCS and CCS. For each experiment, a series of flasks were prepared with 50 mL of dye solution (25–200 mg/L, respectively) and the pH was adjusted from 2 to 8 using a pH meter (Deluxe pH meter, model-101 E). About 0.2 g of the sorbent was added, and the flasks were agitated at 160 rpm. The sorbent was removed by centrifugation and the supernatant was analyzed using a Systronic Spectrophotometer-104 at wavelength of 584 nm.

The amount of dye adsorbed at equilibrium onto carbon, q_e (mg g^{-1}) was calculated by the following mass balance relationship.

$$q_e = (C_0 - C_e)V/W \quad (1)$$

where C_o and C_e are the concentrations (mg L^{-1}) of CV at initial and equilibrium respectively. V is the volume (L) of the solution and W is the weight (g) of the adsorbent used.

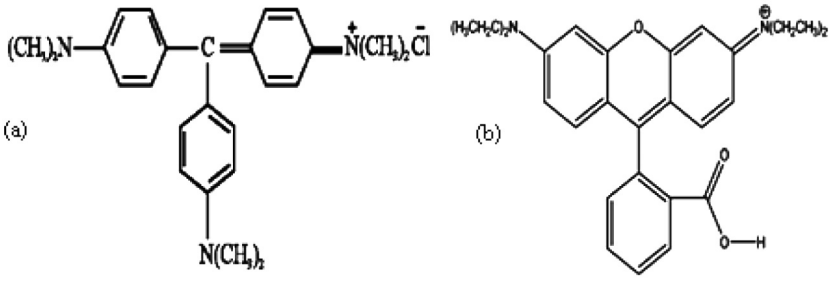

Figure 1 Structure of (a) Crystal violet dye (b) Rhodamine B.

Table 1 Physico-chemical characteristics of RCS and CCS.

Parameters	RCS	CCS
Moisture content (%)	18.74	11.62
Ash content (%)	09.83	12.59
pH	06.68	06.51
Decolorizing power (mg g^{-1})	49.00	47.00
Specific gravity	0.498	1.020
Water soluble matter (%)	05.62	8.072
Conductivity (μs cm^{-1})	0.811	0.922
Zero point charge (pH_{zpc})	4.601	04.00
Apparent density (g mL^{-1})	0.018	0.781
Matter soluble in water (%)	25.78	10.12
Total acidic group	0.1855	0.192

3. Result and discussion

3.1. Characterization of RCS and CCS

Table 1 shows the physico-chemical characteristics of the adsorbents. The moisture content was 18.74% for RCS whereas only 11.62 were observed for CCS. Moisture content not only decreases the adsorption sites but also causes additional weight (Sajjad et al., 2011). The ash content might produce defect (dangling carbon) in the elementary structure of charcoal leading to high adsorption capacity.

3.2. Batch adsorption studies

These studies enabled in determining the optimum operating conditions and to find out the effects of various parameters (like, the initial dye concentration, the solution pH and the contact time) on the percentage removal of dyes. The randomness is increased during adsorption process, resulting in better contact between the adsorbate and adsorbent. Consequently, this led to the enhanced rate of adsorption. The amount of dye adsorbed (mg/g) increased with increasing agitation time and reached equilibrium after 90 min for crystal violet and 80 min for rhodamine B for the initial dye concentration (25–200 mg/L) onto RCS and CCS.

The increase in uptake capacity of the adsorbent with increasing dye concentration may be due to the increase of sorbate quantity. At lower initial dye concentration, sufficient adsorption sites are available for the adsorption of dye ions. Conversely, the numbers of dye ions at higher initial concentration are relatively more as compared to the available adsorption sites. Similar trends are reported by Atmani et al. (2009) for CV onto almond waste and Ali and Muhammad (2008) for CV onto *Calotropis procera*.

The effect of solution pH (range of 2–8) on the amount of removal at a fixed adsorbent dosage (0.2 g) is shown in Fig. 2 for both dyes under consideration. From Fig. 2, it is evident that the maximum removal of color is observed at pH 7 for CV and RH B onto RCS, pH 6 for CV and RH B onto CCS. The percent removal of dyes increases with an increase in the pH and reaches the maximum up to 72.27% for CV onto RCS, 84.98% for CV onto CCS, 81.69% for RH B onto RCS and 90.26% for RH B onto CCS. This may be attributed to the hydrophobic nature of the developed carbon which led to absorb hydrogen ions (H^+) onto the surface of the carbon when

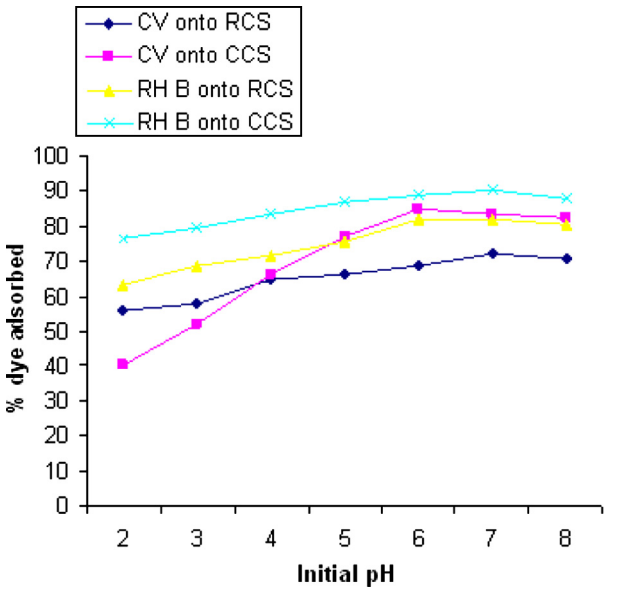

Figure 2 Effect of solution pH for the removal of CV and RH B onto RCS and CCS.

immersed in water and make it positively charged. Low pH value (1.0–3.0) leads to an increase in H^+ ion concentration in the system and the surface of the activated carbon acquires positive charge by absorbing H^+ ions. On the other hand, an increase in the pH value led to the increase in the number of negatively charged sites. As the adsorbent surface is negatively charged at high pH, a significantly strong electrostatic attraction appears between the negatively charged carbon surface and the cationic dye molecule leading to maximum adsorption of CV and RH B from waste water.

The lowest adsorption occurred at pH 2.0 and the greatest adsorption occurred at pH ~6.0 and 7.0. Adsorbent surface would be positively charged up to pH < 4, and heterogeneous in the pH range 4–5. Thereafter, it should be negatively charged. Moreover, the increase in the adsorption of dye with the increasing pH value is also due to the attraction between cationic dye and excess OH^- ions in the solution. The adsorption capacity and rate constant have the tendency to increase as initial pH of the solution increases. This is due to the pH_{zpc} of the adsorbents which has an acidic value; this is favorable for cation adsorption. It is a commonly known fact that the anions are favorably adsorbed by the adsorbent at lower pH values due to the presence of H^+ ions. At high pH values, cations are adsorbed due to the negatively charged surface sites of the adsorbents. The optimum pH value of CV and RH B onto RCS was pH 7 and CV and RH B onto CCS was pH 6.

3.3. Adsorption

In order to optimize the design of an adsorption system to remove the dye, it is important to establish the most appropriate correlations of the equilibrium data of each system (Altinisik et al., 2010). Equilibrium isotherm equations are used to describe the experimental adsorption data. The parameters obtained from the different models provide important information on the adsorption mechanisms, surface properties and affinities of the adsorbent (Bulut et al., 2008). The correlation

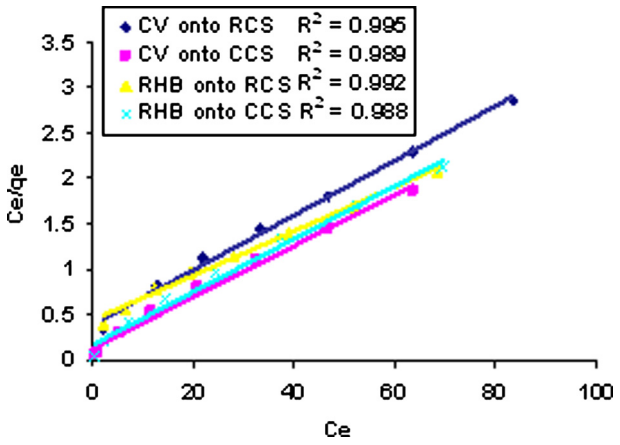

Figure 3 Langmuir isotherm plot for the adsorption of CV and RH B onto RCS and CCS.

with the amount of adsorption and the liquid-phase concentration was tested with the Langmuir, Freundlich, Dubinin Radushkevich and Temkin adsorption isotherm equations. Linear regression is frequently used to determine the best-fitting isotherm, and the applicability of isotherm equations is compared by judging the correlation coefficients.

The Langmuir isotherm theory assumes monolayer coverage of adsorbate over a homogeneous adsorbent surface (Langmuir, 1918). Once a metal molecule occupies a site, no further adsorption can take place at that site. It is commonly expressed as follows:

$$q_e = (Q_m K_a C_e)/(1 + K_a C_e) \quad (2)$$

The Langmuir isotherm Eq. (2) can be linearized into the following form (Kinniburgh, 1986).

$$C_e/q_e 1/K_a Q_m + (1/Q_m \times C_e) \quad (3)$$

where q_e and C_e are defined before in Eq. (1), Q_m is a constant, reflecting a complete monolayer (mg g^{-1}); K_a is the adsorption equilibrium constant (L mg^{-1}) that is related to the apparent energy of sorption. A plot of C_e/q_e versus C_e (Fig. 3) should indicate a straight line of slope $1/Q_m$ and an intercept of $1/(K_a Q_m)$.

The results obtained from the Langmuir model are shown in Table 2. The sorption capacities of RCS and CCS for the selected dyes are followed the order: 40.81 mg/g (RH B onto RCS) > 35.34 mg/g (CV onto CCS) > 34.01 mg/g (RH B onto CCS) > 33.22 mg/g (CV onto RCS). Sorption capacities of low cost adsorbents for various dyes are reported by other researchers and are presented in Table 3, for comparison. From the values, we conclude that the maximum adsorption corresponds to a saturated monolayer of adsorbate molecules. The correlation coefficient ($R^2 > 0.9880$) showed strong positive evidence on the adsorption which follows the Langmuir isotherm.

The Freundlich isotherm (Freundlich, 1960) can be applied to non-ideal adsorption on heterogeneous surfaces as well as multilayer sorption. The Freundlich isotherm can be derived assuming a logarithmic decrease in the enthalpy of adsorption with the increase in the fraction of occupied sites and is commonly given by the following non-linear equation:

$$q_e = K_F C_e^{1/n} \quad (4)$$

Eq. (4) can be linearized in the logarithmic form (Eq. (5)), and the Freundlich constants can be determined:

$$\log q_e = \log K_F + \frac{1}{n} \log C_e \quad (5)$$

A plot of log q_e versus log C_e enables to determine the constants K_f and $1/n$. K_f is roughly an indicator of the adsorption capacity, related to the bond energy, and $1/n$ is the adsorption intensity of dyes onto the adsorbent of surface heterogeneity. The magnitude of the exponent, $1/n$, gives an indication of the favorability of adsorption. A value for $1/n$ below one indicates a normal Langmuir isotherm, while $1/n$ above one is

Table 2 Isotherm constants for adsorption of CV and RH B onto RCS and CCS.

Isotherm model	CV		RH B	
	RCS	CCS	RCS	CCS
Langmuir				
Q_m (mg g^{-1})	33.22	35.33	40.82	34.01
b (L mg^{-1})	0.076	0.216	0.057	0.174
R^2	0.995	0.989	0.992	0.988
Freundlich				
$1/n$	0.433	0.310	0.517	0.303
K_f (mg g^{-1})	4.785	9.990	4.085	9.051
R^2	0.982	0.966	0.988	0.972
Dubinin-Radushkevich				
Q_m (mg g^{-1})	21.67	25.40	23.26	23.59
K ($\times 10^{-5}$ mol^2 kJ^{-2})	1×10^{-06}	1×10^{-07}	-2×10^{-06}	8×10^{-08}
E (kJ mol^{-1})	0.707	2.236	0.5	2.5
R^2	0.762	0.830	0.748	0.674
Temkin				
α (L g^{-1})	1.032	60.15	0.417	4.295
β (kJ mol^{-1})	6.523	5.304	8.302	5.162
R^2	0.989	0.981	0.977	0.924

Table 3 Reported maximum adsorption capacities (Q_m in mg g^{-1}) in the literature for cationic dye obtained on low-cost adsorbents.

Adsorbent	Q_m(mg g^{-1})	References
RH B onto RCS	40.82	This study
CV onto CCS	35.33	This study
RH B onto CCS	34.01	This study
CV onto RCS	33.22	This study
Luffa cylindrical	9.920	Temkin and Pyzhey (1940)
Coffee ground activated carbon	23.00	Santhi et al. (2010)
Kolin	5.44	Gupta et al. (2008)
Wheat bran	22.73	Gupta et al. (2007)
Rice bran	14.63	Gupta et al. (2007)
Hen feathers	26.10	Mittal (2006)
Arundo donax root carbon	8.69	Zhang et al. (2008)
Bentonite	7.72	Tahir and Rauf (2006)

indicative of cooperative adsorption (Fytianos et al., 2000). It is lower than the experimental amounts corresponding to the adsorption isotherm plateau, which is unacceptable.

The D–R isotherm was also applied to estimate the porosity apparent free energy and the characteristics of adsorption (Dubinin, 1960; Radushkevich, 1949). It can be used to describe adsorption on both homogenous and heterogeneous surfaces (Shahwan and Erten, 2004). The D–R equation can be defined by the following equation.

$$\ln q_e = \ln Q_m - K\varepsilon^2 \tag{6}$$

where K is a constant related to the adsorption energy, Q_m is the theoretical saturation capacity, and ε is the Polanyi potential, calculated from Eq. (7),

$$\varepsilon = RT\ln\left(1+\frac{1}{C_e}\right) \tag{7}$$

where C_e is the equilibrium concentration of dyes (mol L^{-1}), R is the gas constant (8.314 J mol^{-1} K^{-1}), and T is the temperature (K). By plotting ln q_e versus ε^2, it is possible to determine the value of K from the slope and the value of Q_m (mg g^{-1}) from the intercept. The mean free energy E (kJ mol^{-1}) of sorption can be estimated by using K values as expressed in the following equation (Hobson, 1969).

$$E = \frac{1}{\sqrt{2K}} \tag{8}$$

The parameters obtained using the above equations are summarized in Table 2. The E value calculated using Eq. (8) indicating that the physical adsorption plays a significant role in the uptake of CV and RH B onto RCS and CCS (Hobson, 1969).

Temkin and Pyzhey (1940) considered the effects of some indirect adsorbate or adsorbate interactions on adsorption isotherms and suggested that because of these interactions the heat of adsorption of all the molecules in the layer would decrease linearly with coverage. The Temkin isotherm has commonly been applied in the following form:

$$q_e = \frac{RT}{b}\ln(AC_e) \tag{9}$$

The Temkin isotherm Eq. (9) can be simplified to the following equation,

$$q_e = \beta\ln\alpha + \beta\ln C_e \tag{10}$$

where

$$\beta = (RT)/b \tag{11}$$

The constant β is related to the heat of adsorption (Pearce et al., 2003). The adsorption data were analyzed according to the linear form of Temkin isotherm Eq. (10). The linear isotherm constants and coefficients of determination are presented in Table 2. The correlation coefficients R^2 obtained from Temkin model were comparable to that obtained for Langmuir and Freundlich and D–R equations, which explain the applicability of Temkin model to the adsorption of CV and RH B onto RCS and CCS.

It can be seen that the Langmuir isotherm fits the data better than Freundlich, D–R, and Temkin isotherms. The fact that it may be due to the predominantly homogeneous distribution of active sites on the activated carbons surfaces; since the Langmuir equation assumes that the adsorbent surface is energetically homogeneous. This is also confirmed by the high value of R^2 in case of Langmuir. The maximum sorption capacity (Q_m) of the adsorption of CV and RH B onto RCS and CCS was compared with those reported in the literature (Table 3).

3.4. Adsorption kinetics

The study of adsorption kinetics describes the solute uptake rate and evidently this rate controls the residence time of the adsorbate at the solid solution interface. The rate of sorption can be computed from the kinetic study. In order to investigate the mechanism of sorption and potential rate controlling steps, several models have been developed. Thus, the kinetics were analyzed using pseudo-first-order (Lagergren, 1898), pseudo-second-order (Ho et al., 2000), Elovich (Chien and Clayton, 1980; Zeldowitsch, 1934) and intraparticle diffusion (Weber and Morris, 1963) kinetic models. The conformity between experimental data and the model-predicted values was expressed by the correlation coefficients (R^2, values close or equal to 1).

The pseudo first-order equation of Lagergren is generally expressed as follows:

$$\frac{dq_t}{d_t} = K_1(q_e - q_t) \tag{12}$$

where q_e and q_t are the adsorption capacity at equilibrium and at time t, respectively (mg g^{-1}), K_1 is the rate constant of pseudo-first-order adsorption (L min^{-1}). Integrating Eq. (12) for the boundary conditions $t = 0 - t$ and $q_t = 0 - q_t$ gives

$$\log\left(\frac{q_e}{q_e - q_t}\right) = \frac{K_1}{2.303}t \tag{13}$$

Eq. (13) can be rearranged to obtain the following linear form:

$$\log(q_e - q_t) = \log(q_e) - \frac{K_1}{2.303}t \tag{14}$$

The values of q_e and K_1 for the pseudo-first-order kinetic model were determined from the intercepts and the slopes of the plots of log ($q_e - q_t$) versus time. The K_1 values, R^2 values and q_e values (experimental and calculated) are summarized in Table 4.

Table 4 First-and second-order kinetic parameters for the adsorption of CV and RHB onto RCS and CCS at different initial concentration.

System	C_o (mg/L)	$q_{e\ (exp)}$ (mg/g)	Pseudo-first-order			Pseudo-second-order		
			K_1 (min)	$q_{e(cal)}$ mg/g	R^2	K_2 (g/mg min)	$q_{e(cal)}$ mg/g	R^2
CV onto RCS	50	11.83	0.058	3.375	0.958	0.04	12.077	0.9999
	100	19.76	0.054	7.356	0.886	0.016	20.325	0.9995
	150	26.78	0.032	4.876	0.585	0.016	27.027	0.9989
	200	30.36	0.052	8.180	0.696	0.015	30.864	0.9994
CV onto CCS	50	11.87	0.036	4.175	0.518	0.019	12.091	0.9956
	100	20.37	0.023	2.017	0.866	0.024	20.491	0.9995
	150	27.91	0.026	1.236	0.883	0.054	28.011	0.9999
	200	33.11	0.023	1.171	0.929	0.053	33.222	1.0000
RH B onto RCS	50	10.86	0.065	3.417	0.943	0.035	11.173	0.9993
	100	21.68	0.064	5.215	0.914	0.031	21.978	0.9998
	150	27.65	0.066	6.884	0.922	0.023	28.089	0.9998
	200	32.88	0.055	4.655	0.931	0.028	33.222	0.9999
RH B onto CCS	50	12.62	0.066	6.889	0.928	0.024	13.037	0.9977
	100	22.83	0.065	16.77	0.656	0.010	23.529	0.9970
	150	29.88	0.044	7.629	0.674	0.013	30.303	0.9986
	200	35.29	0.058	5.833	0.800	0.026	35.587	0.9999

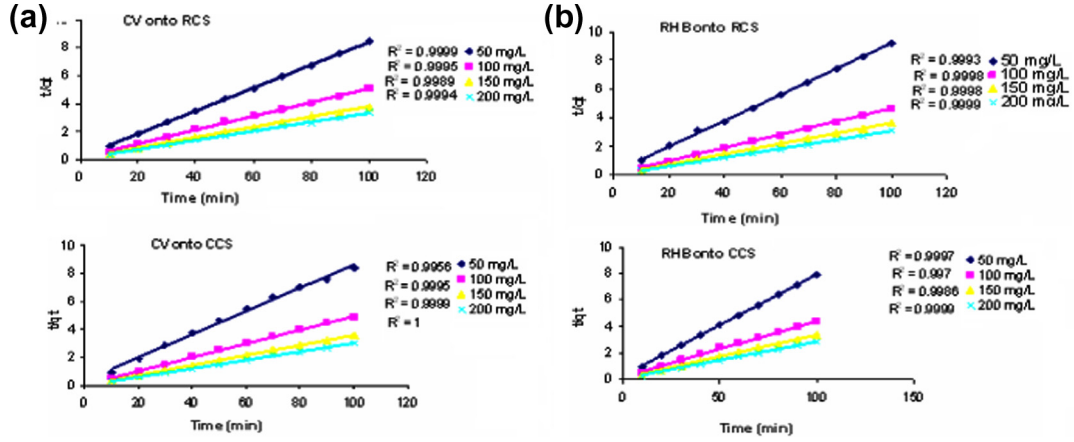

Figure 4 Pseudo second-order kinetics at different initial concentrations for (a) CV onto RCS and CCS (b) RH B onto RCS and CCS.

The pseudo-second order equation is generally given as follows:

$$\frac{dq_t}{d_t} = K_2(q_e - q_t)^2 \tag{15}$$

where K_2 (g(mg min)$^{-1}$) is the second-order rate constant of adsorption. Integrating Eq. (15) for the boundary conditions $q_t = 0 - q_t$ at $t = 0 - t$ is simplified as can be rearranged and linearized to obtain:

$$\frac{t}{q_t} = \frac{1}{K_2 q_e^2} + \frac{1}{q_e}(t) \tag{16}$$

The second-order rate constants were used to calculate the initial sorption rate, given by the following equation:

$$h = K_2 q_e^2 \tag{17}$$

The plot of t/q_t versus time is a straight line as shown in Fig. 4. The K_2 and q_e values determined from the slopes and intercepts of the plot are presented in Table 4 along with the corresponding correlation coefficient.

The Elovich equation is another rate equation based on the adsorption capacity generally expressed as follows.

$$\frac{dq_t}{dt} B_E \exp(-A_{Eqt}) \tag{18}$$

where B_E is the initial adsorption rate (mg(g min)$^{-1}$) and A_E is the desorption constant (g mg^{-1}) during any experiment.

It is simplified by assuming $A_E B_E t \gg t$ and by applying the boundary conditions $q_t = 0$ at $t = 0$ and $q_t = q_t$ at $t = t$ Eq. (18) becomes:

$$q_t = \frac{1}{A_E} \ln(B_E A_E) + \frac{1}{A_E} \ln(t) \tag{19}$$

A plot of q_t versus $\ln(t)$ should yield a linear relationship with a slope of $(1/A_E)$ and an intercept of $(1/A_E) \ln (A_E B_E)$. Thus, the constants can be obtained from the slope and the intercept of the straight line is mentioned in Table 5.

Table 5 Parameters of the Elovich and intra particle diffusion model for the adsorption of CV and RH B onto RCS and CCS.

System	C_o	Elovich model			Intraparticle diffusion Model		
	(mg/L)	A_E	B_E	R^2	K_{dif}	C	R^2
CV onto RCS	50	1.642	1.9×10^6	0.969	0.193	10.08	0.9136
	100	0.814	1.2×10^5	0.961	0.399	16.03	0.9522
	150	1.028	5.7×10^9	0.853	0.332	23.23	0.9298
	200	0.978	6.6×10^{10}	0.845	0.350	26.85	0.9282
CV onto CCS	50	1.524	2.6×10^5	0.740	0.230	9.326	0.8557
	100	1.895	1.8×10^{14}	0.821	0.183	18.38	0.9277
	150	2.996	5.1×10^{33}	0.934	0.111	26.75	0.982
	200	2.982	1.7×10^{40}	0.925	0.113	31.91	0.985
RH B onto RCS	50	1.490	8.8×10^4	0.812	0.216	8.931	0.7879
	100	1.536	2.1×10^{12}	0.907	0.215	19.67	0.9342
	150	1.116	2.4×10^{11}	0.859	0.298	24.89	0.8886
	200	1.325	6.7336	0.922	0.249	30.55	0.9406
RH B Onto CCS	50	1.094	1.1×10^4	0.987	0.293	9.948	0.9496
	100	0.717	1.2×10^{11}	0.771	0.460	18.13	0.8783
	150	0.898	3.5×10^9	0.796	0.383	25.89	0.8832
	200	1.392	1.4764	0.912	0.241	32.96	0.9630

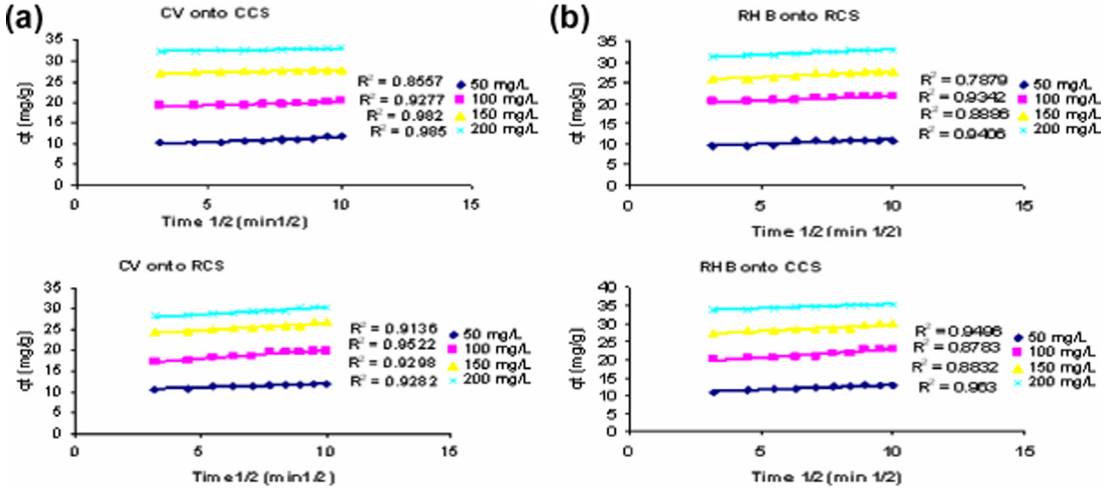

Figure 5 Intra particle diffusion plot at different initial dye concentrations for CV and RH B onto RCS and CCS.

When the diffusion (internal surface and pore diffusion) of dye molecule inside the adsorbent is the rate-limiting step, then adsorption data can be presented by the following equation:

$$q_t = K_{dif} t^{1/2} + C \tag{20}$$

where C (mg g^{-1}) is the intercept and K_{dif} (mg g^{-1} min$^{-1/2}$) is the intraparticle diffusion rate constant. The values of qt were found to be linearly correlated with values of $t^{1/2}$ and the rate constant K_{dif} directly evaluated from the slope of the regression line (Table 5).

The fitted linear regression plots showed that the experimental data had its best fit with the pseudo-second-order model for all four investigated concentrations with higher determination coefficients ($R^2 > 0.995$) than those of the pseudo-first-order model and Elovich model. Therefore, it is found that the rate of CV and RH B adsorption onto RCS and CCS is of pseudo-second-order, suggesting that the adsorption of dye onto adsorbents is influenced by both the dye and the adsorbent concentrations under the investigated conditions (Abramian and El-Rassy, 2009). The fitted linear regression plots of pseudo-second-order model are shown in Fig. 5. In addition, the experimental adsorption capacity ($q_{e\ (exp)}$) values were very close to the model-calculated adsorption capacity ($q_{e\ (cal)}$) data (Table 4), verifying the high correlation of adsorption to the pseudo-second-order model.

Intraparticle diffusion was analyzed using Eq. (20). The plots of intraparticle diffusion of CV and RHB onto RCS and CCS at the initial concentrations of 50, 100, 150, 200 mg/L are illustrated in Fig. 5. Referring to Fig. 5, the linearity of the plots demonstrated that intraparticle diffusion played a significant role in the uptake of CV and RH B. However, there is no sufficient indication about it. The author Ho (Ho, 2003) has shown that if the intraparticle diffusion is the sole rate-limiting step, it is essential for the qt versus $t^{1/2}$ plots

to pass through the origin, which is not the case in Fig. 5, it may be concluded that boundary layer diffusion and intraparticle diffusion were concurrently operating during the adsorbate and adsorbent interactions.

4. Conclusion

The results revealed the potential of *C. sativus* an agricultural solid waste, to be a low-cost adsorbent for removing CV and RH B from aqueous solutions. The adsorption was dependent on the initial pH, contact time and dye concentration. Equilibrium data agreed well with Langmuir isotherm model and the kinetic modeling study has shown that the experimental data were found to follow the pseudo-second-order model suggesting a chemisorption process. The result of the intra particle diffusion model suggested that intra particle diffusion was not the only rate controlling step. This study proved that the eco friendly adsorbents RCS and CCS showed a better performance and the raw material *C. sativus* is easily available in large quantity and its treatment method is very economical.

References

Abramian, L., El-Rassy, H., 2009. Adsorption kinetics and thermodynamics of azo-dye Orange II onto highly porous titania aerogel. Chem. Eng. J. 150, 403–410.

Ali, H., Muhammad, S.K., 2008. Biosorption of Crystal violet from water on leaf biomass of *Calotropis procera*. J. Environ. Sci. Technol. 1 (3), 143–150.

Altinisik, A., Gur, Emel, Seki, Yoldas, 2010. A natural sorbent, *Luffa cylindrical* for the removal of a model basic dye. J. Hazard Mater., http://dx.doi.org/10.1016.

Atmani, F., Bensmaili, A., Mezenner, N.Y., 2009. Synthetic textile effluent removal by skin almonds waste. J. Environ. Sci. Technol. 2 (4), 153–169.

Bulut, E., Ozacar, M., Sengil, A.I., 2008. Adsorption of malachite green onto bentonite: equilibrium and kinetic studies and process design. Micropore Mesopre Mater. 115, 234–246.

Chien, S.H., Clayton, W.R., 1980. Application of Elovich equation to the kinetics of phosphate release and sorption on soils. Soil Sci. Soc. Am. J. 44, 265–268.

Dubinin, M.M., 1960. The potential theory of adsorption of gases and vapors for adsorbents with energetically non-uniform surface. Chem. Rev. 60, 235–266.

Forgacs, E., Cserhatia, T., Oros, G., 2004. Removal of synthetic dyes from waste water. A review. Environ. Int. 30, 953–971.

Freundlich, H., 1960. Uber die adsorption in losungen (Adsorption in solution). Z. Phys. Chem. 57, 384–470.

Fytianos, K., Voudrias, E., Kokkalis, E., 2000. Sorption desorption behavior of 2,4-dichlorophenol by marine sediments. Chemosphere 40, 3–6.

Gupta, V.K., Ali, I., Saini, V.K., 2007. Adsorption studies on the removal of vertigo blue 49 and orange DNA 13 from aqueous solutions using carbon slurry developed from a waste material. J. Colloid Interface Sci. 315, 87–93.

Gupta, V.K., Mittal, A., Krishnan, L., Mittal, J., 2008. Adsorption of basic Fuchsine using waste materials-bottom ash and de-oiled soya as adsorbents. J. Colloid Interface Sci. 319, 30–39.

Sajjad, Haidera, Nausheen, B., Soo, Y.P., Yousaf, Iqbald, Waheed Al-Masrya, A., 2011. Adsorption of bromo-phenol blue from an aqueous solution onto thermally modified granular charcoal. Chem. Eng. Res. Design. 89, 23–28.

Ho, Y.S., 2003. Removal of copper ions from aqueous solution by tree fern. Water Res. 37, 2323–2330.

Ho, Y.S., McKay, G., Wase, D.A.J., Foster, C.F., 2000. Study of the sorption of divalent metal ion onto peat. Adsorp. Sci. Technol. 18, 639–650.

Hobson, J.P., 1969. Physical adsorption isotherms extending from ultrahigh vacuum to vapor pressure. J. Phys. Chem. 73, 2720–2727.

Kaur, Sumanjit, Lark, B.S., Kumar, Pravin, 1998. Chemical oxygen demand reduction of some dyes using fly ash an adsorbent. J. Environ. Poll. 5, 59–66.

Kinniburgh, D.G., 1986. General purpose adsorption isotherms. Environ. Sci. Technol. 20, 895–904.

Lagergren, S., 1898. Zur theorie dersogenannten adsorption geloster stoffe kungliga svenska vetenskapsakademiens. Handlingar 24, 1–39.

Langmuir, I., 1918. The adsorption of gases on plane surface of glass, mica and platinum. J. Am. Chem. Soc. 40, 1361–1403.

Mecay, G., Allen, S.J., Mc Concey, I.P., Wallters, J.H.R., 1984. External mass transfer and homogeneous solid-phase diffusion effects during the adsorption of dyestuffs. Ind. Eng. Chem. Process Design Dev. 23 (2), 221–226.

Meshko, V., Morcovaska, L., Minkcheva, M., Cibulic, V., 1998. Fixed bed adsorption column design for purification of waste water from textile fibres colouring. J. Ser. Chem. Soc. 63 (11), 891–901.

Mittal, A., 2006. Adsorption kinetics of removal of a toxic dye, malachite green, from waste water by using hen feathers. J. Hazard. Mater. B 133, 196–202.

Pearce, C.I., Lioyd, J.R., Guthrie, J.T., 2003. The removal of dye from textile waste water using whole bacterial cells: a review. Dyes Pigm. 58, 179–196.

Radushkevich, L.V., 1949. Potential theory of sorption and structure of carbons. Zh. Fiz. Khim. 23, 1410–1420.

Santhi, T., Manonmani, S., 2010. Removal of methylene blue from aqueous solution by activated carbon prepared from the peel of cucumis sativa fruit by adsorption. Bioresources.com 5 (1), 419–437.

Santhi, T., Manonmani, S., 2011. Removal of malachite green from aqueous solution by activated carbon prepared from the peel of cucumis sativa fruit by adsorption. Clean, Air, Soil, Water 39 (2), 162–170.

Santhi, T., Manonmani, S., Smitha, T., 2010. Removal of malachite green from aqueous solution by activated carbon prepared from the epicarp of *Ricinus communis* by adsorption. J. Hazard Mater. 179 (1–3), 178–186.

Shahwan, T., Erten, H.N., 2004. Temperature effects on barium sorption on natural kalinite and chlorite-illite clays. J. Radioanal. Nucl. Chem. 260, 43–48.

Tahir, S.S., Rauf, N., 2006. Removal of cationic dye from aqueous solution by adsorption onto bentonite clay. Chemosphere 63, 1842–1848.

Temkin, M.J., Pyzhey, V., 1940. Recent modifications to Langmuir isotherms. Acta Physiochim. USSR 12, 217–222.

Voundrias, E., Fytianos, K., Bozani, E., 2002. Sorption–desorption isotherms of dyes from aqueous solutions and wastewaters with different sorbent materials. Globle Nest. Int. J. 4, 75–83.

Weber, W.J., Morris, J.C., 1963. Kinetics of adsorption on carbon from solution. J. Sanity Eng. Div. Am. Soc. Civil Eng. 89, 31–59.

Wong, Y.C., Szeto, Y.S., Cheung, W.H., Mckay, G., 2004. Adsorption of acid dyes on chitosan-equilibrium isotherm analyses. Process. Biochem. 39, 695–704.

Zeldowitsch, J., 1934. Über den mechanismus der katalytischen oxidation von CO an MnO_2. Acta Physicochim. URSS 1, 364–449.

Zhang, J., Li, Y., Zhang, C., Jing, Y., 2008. Adsorption of malachite green from aqueous solution onto carbon prepared from Arundo donax root. J. Hazard. Mater. 150, 774–782.